journal

J. Am. Ceram. Soc., 0 [2] 624–628 (2015)
DOI: 10.1111/jace.13318

Glass-Like Thermal Conductivity of (010)-Textured Lanthanum-Doped Strontium Niobate Synthesized with Wet Chemical Deposition

Brian M. Foley,[‡,*,†] Harlan J. Brown-Shaklee,[§,*] Michael J. Campion,[§] Douglas L. Medlin,[¶] Paul G. Clem,[§,*] Jon F. Ihlefeld,[§,*] and Patrick E. Hopkins[‡,*]

[‡]Department of Mechanical and Aerospace Engineering, University of Virginia, Charlottesville, Virginia 22904

[§]Electronic, Optical and Nano Materials Department, Sandia National Laboratories, Albuquerque, New Mexico 87185

[¶]Materials Physics Department, Sandia National Laboratories, Livermore, California 94550

We have measured the cross-plane thermal conductivity (κ) of (010)-textured, undoped, and lanthanum-doped strontium niobate ($Sr_{2-x}La_xNb_2O_{7-\delta}$) thin films via time-domain thermoreflectance. The thin films were deposited on (001)-oriented $SrTiO_3$ substrates via the highly-scalable technique of chemical solution deposition. We find that both film thickness and lanthanum doping have little effect on κ, suggesting that there is a more dominant phonon scattering mechanism present in the system; namely the weak interlayer-bonding along the *b*-axis in the $Sr_2Nb_2O_7$ parent structure. Furthermore, we compare our experimental results with two variations of the minimum-limit model for κ and discuss the nature of transport in material systems with weakly-bonded layers. The low cross-plane κ of these scalably-fabricated films is comparable to that of similarly layered niobate structures grown epitaxially.

I. Introduction

The development of materials with exceptionally low thermal conductivities (κ) has been an exciting area of research over the past decade.[1–7] Materials that possess such extreme attributes provide unique opportunities to study both the fundamental physics of carrier transport and also create new solutions to challenging engineering problems. Nanostructuring has proven to be an effective way of minimizing the value of κ through several extrinsic mechanisms, including superlattices, nano-grains, crystallographic texture, quantum dots, etc.[8–16] As a result, these nano-structured material systems have garnered significant interest as both thermoelectric (TE) materials and as thermal barrier coatings.

While the demonstrated reduction of κ through the use of these nano-structures has yielded promising results, the atomic-layer-based deposition processes used to fabricate many of these structures may limit their commercial-influence to niche markets where cost is not the most important design factor.[17] Ideally, these materials will be able to be produced in large quantities both quickly and inexpensively so as to maximize their applicability and commercial potential. To that end, bulk nano-structured materials, or nano-composites, are an intriguing class of materials which can be fabricated via scalable manufacturing processes while retaining their thermally insulative properties.[10,11,14-16] In addition to manufacturability, the ideal materials also should be stable against Ostwald ripening at operation temperatures and therefore may limit the utility of many nano-structured and nano-composite systems. Therefore, the selection of materials that spontaneously form natural, thermodynamically stable, nano-structures is desirable.

Recent attention has been paid to the naturally layered oxides[18–22] as a class of crystalline materials with very low, glass-like thermal conductivities. One such material that has garnered interest of late is the $Sr_2Nb_2O_7$ material system.[19–21] $Sr_2Nb_2O_7$ is an orthorhombic perovskite phase (space group #36-*Cmc*21) composed of octahedrally coordinated niobium and 12-coordinated strontium, separated by a SrO double layer in the cross-plane direction [23] (i.e., in the standard setting, the direction perpendicular to the layers and referred to as the *b*-axis direction in this work, but also called the *c*-axis in the nonstandard setting). It has been shown that the power factor is increased due to introduction of charge carriers with lanthanum doping,[19–21] suggesting that it may be well suited for thermoelectric applications. Furthermore, the naturally layered structure of this material is the equilibrium crystal structure, meaning it is a very stable configuration that is ideally suited for high-temperature applications.

Given the layered structure in this class of compounds, it is interesting to ask whether the thermal transport behavior is sensitive to film boundary and/or impurity scattering effects, or whether the internal layering will dominate the thermal transport. In this work, we use time-domain thermoreflectance (TDTR) to measure the cross-plane (*b*-axis) lattice thermal conductivity of a series of lanthanum-doped strontium niobate ($Sr_{2-x}La_xNb_2O_{7-\delta}$) thin films of varying thicknesses. The films were fabricated through chemical solution deposition[24,25] (CSD), which is a scalable technique for producing large quantities of material both quickly and inexpensively.[26] We find that neither film thickness nor doping lead to further reductions in κ, suggesting that phonon scattering at the weakly bonded layer interfaces is the dominant scattering mechanism that dictates thermal transport in layered perovskite structured strontium niobate. The results of the measurements are analyzed in the context of a minimum-limit model for thermal conductivity.

II. Experimental Procedure

(0*k*0)-oriented fiber-textured strontium niobate and lanthanum-doped strontium niobate films were prepared on $SrTiO_3$ substrates as described in previous work.[27] In short, a chelate-based CSD approach was used where strontium or strontium and lanthanum acetates were dissolved in propionic acid and niobium butoxide was chelated with six molar equivalents of acetic acid. The appropriate amount of the dissolved acetates was added to the niobium precursor, as measured by constituent masses, and the solutions were diluted to 0.15*M* with anhydrous ethanol. Solutions were

M. White—contributing editor

Manuscript No. 34638. Received March 25, 2014; approved October 2, 2014.
*Member, The American Ceramic Society.
[†]Author to whom correspondence should be addressed. e-mail: bmf4su@virginia.edu

spin cast onto (001)-oriented $SrTiO_3$ single crystalline substrates at 3000 rpm for 30 s and pyrolyzed on a hot plate in air at 300°C for 5 min. $Sr_2Nb_2O_7$ and $Sr_{1.9}La_{0.1}Nb_2O_{7-\delta}$ films were formed by annealing the as-pyrolyzed films to 1000°C in an air atmosphere for 5 min by directly inserting the samples into a preheated furance. After the final deposition and crystallization anneal, the La-containing films were postannealed in a dry 3% H_2/N_2 atmosphere to promote solubility of the lanthanum and to activate electronic carriers for thermoelectric applications. The coating/pyrolysis/crystallization process was repeated to increase film thickness with as-crystallized individual layer thickness of 27 nm.

The phase-assemblage and orientation of the films was confirmed via x-ray diffraction (XRD; Philips MPD, PANalytical, Westborough, MA) using CuK_α radiation. Scanning transmission electron microscopy (STEM) images were generated using an FEI-Titan G2 instrument (FEI, Hillsboro, OR), operated at 200 keV and equipped with a high angle annular dark field (HAADF) detector. The thermal conductivities of the samples were determined using TDTR[28] where we fit the experimental data to a multi-layer thermal model.[29–31] To provide the transducer for our optical measurements, we deposited an aluminum film on the samples by electron beam evaporation. The film was approximately 90 nm thick, as confirmed by picosecond ultrasonics.[32,33] For this experiment, we modulate the pump-beam using a linearly amplified 11.39 MHz sinusoid and monitor the ratio of the in-phase to out-of-phase signals from the probe beam using a lock-in amplifier (Stanford Research Systems 844, Sunnyvale, CA). Additionally, we assume literature values for the heat capacities of Al [Ref. (34)] and $Sr_2Nb_2O_7$ [Ref. (35)], as well as the bulk thermal properties of $SrTiO_3$ [Refs. (36,37)].

III. Results and Discussion

Figure 1(a) shows a representative group of X-ray diffraction (XRD) patterns for $Sr_{2-x}La_xNb_2O_{7-\delta}$ films of various thicknesses doped with 5% lanthanum ($x = 0.1$). XRD reveals highly (0k0)-oriented films for each thickness. Minority peaks associated with the 002 and 151 reflections were also observed, but constituted less than 3% of the diffracting volume based upon comparison of measured intensities and those expected from a random powder pattern. In previous work[27] these films were shown to possess a random in-plane orientation and therefore are fiber-textured. Also, while we utilize single crystalline substrates in this study, (010)-fiber texture was identified on non-lattice-matched and polycrystalline substrates, demonstrating a preferred (010) out-of-plane orientation regardless of substrate,[27] which makes this technique/materials system uniquely manufacturable for thermal applications.

Figure 1(b) is comprised of atomic-resolution HAADF-STEM images illustrating the layered crystal structure of strontium niobate. The left image depicts the interface between the thin film and $SrTiO_3$ substrate, confirming that the layers are well aligned with the substrate. The right image in Fig. 1(b) shows detail of an individual $Sr_2Nb_2O_7$ grain that was tilted, in the microscope, to a ⟨101⟩-type orientation, allowing the layered structure to be imaged directly. These observations identify the presence of defects in the layering sequence. In the ideal $Sr_2Nb_2O_7$ crystal structure, the NbO_6-octahedra are arranged in slabs that are 4-octahedra wide along the b-axis.[23,38] However, more generally within the $Sr_nNb_nO_{3n+2}$ homologous series (for which $Sr_2Nb_2O_7$ corresponds to $n = 4$), slab widths of both 4 and 5 NbO_6-octahedra have been observed[39,40]; for instance, the $Sr_5Nb_5O_{17}$ structure (the $n = 5$ member of the homologous series) consists entirely of slabs that are 5 octahedra-wide.[41] Examples of individual $n = 4$ and 5 slabs are indicated on Fig. 1(b) with the superimposed Sr and Nb atom positions from ⟨101⟩ projections of $Sr_2Nb_2O_7$ and $Sr_5Nb_5O_{17}$. The arrows on Fig. 1(b) indicate the distribution of $n = 5$ slabs across one grain.

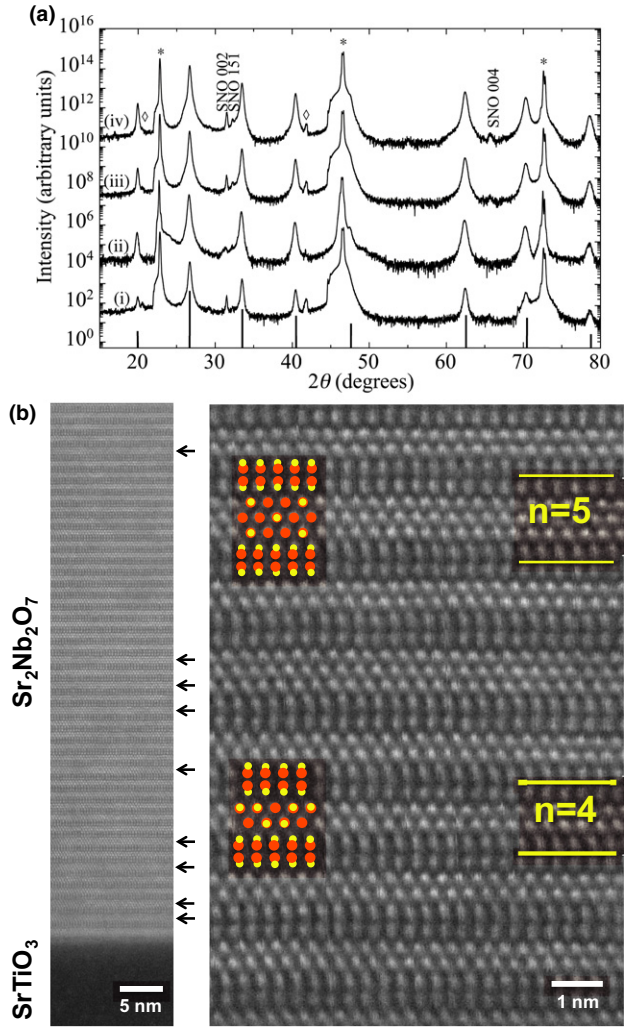

Fig. 1. (a) X-ray diffraction patterns of samples with 5 % lanthanum ($x = 0.1$) and the following thicknesses (nm); (i) 130, (ii) 220, (iii) 400, (iv) 800. The bar markers along the horizontal axis indicate the 2θ angles of the (0k0) reflections, while * denotes reflections from substrate planes and ◦ denotes substrate reflections from CuK_β radiation. (b) Atomic-resolution HAADF-STEM images illustrating the layered crystal structure of strontium niobate. The grain is imaged along a ⟨101⟩ type direction with the b-axis normal to the $SrTiO_3$ substrate. Arrows along the left image indicate the position of defects in the layering sequence. The image on the right shows a higher magnification of a section of the grain overlaid with ⟨101⟩ projections of the Sr (yellow) and Nb (orange) atom positions in the $Sr_2Nb_2O_7$ ($n = 4$ NbO_6 octahedra) and $Sr_5Nb_5O_{17}$ ($n = 5$ NbO_6 octahedra) crystal structures.

At this defect density (9 slabs of the $n = 5$ phase versus 34 slabs of $n = 4$ present within the left image), we calculate that there is a small amount of oxygen reduction by $\delta = 0.05$ in the $Sr_{2-x}La_xNb_2O_{7-\delta}$ samples. To confirm our results were not sensitive to this low level of reduction, an additional sample ($x = 0.1$, approximately 220 nm thick) was prepared through CSD, but done so in oxidizing atmospheres to discourage the formation of the $n = 5$ slabs.[27]

Figure 2 shows the measured thermal conductivities of our $Sr_{2-x}La_xNb_2O_{7-\delta}$ thin films as a function of both film thickness ($x = 0.1$) and doping with lanthanum (constant film thickness) at room temperature. The error bars encompass the uncertainty in the thickness of the 90 nm aluminum film deposited on the samples to serve as a transducer for the optical measurement, as well as the standard deviation about the mean for the three measurements made on each sample. Measurement of the single sample prepared in oxidizing atmospheres yielded a thermal conductivity of 0.60 W· (m · K)$^{-1}$

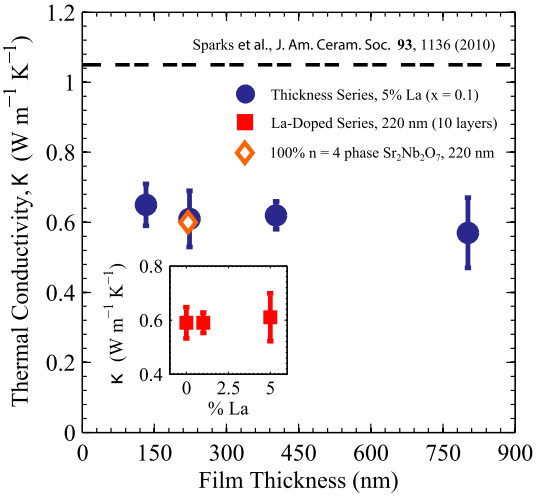

Fig. 2. Thermal conductivities of CSD-fabricated $Sr_{2-x}La_xNb_2O_{7-\delta}$ thin films as a function of film thickness (circles) with 5% La ($x = 0.1$), as well as doping with Lanthanum (squares, inset) for a fixed film thickness of approximately 220 nm, along with the thermal conductivity of bulk, hot-forged $Sr_2Nb_2O_7$ along the *b*-axis reported by Sparks *et al.* (dashed line). The thermal conductivity exhibits little dependence on both the thickness and dopant level, suggesting that there is a more dominant scattering mechanism present in the material.

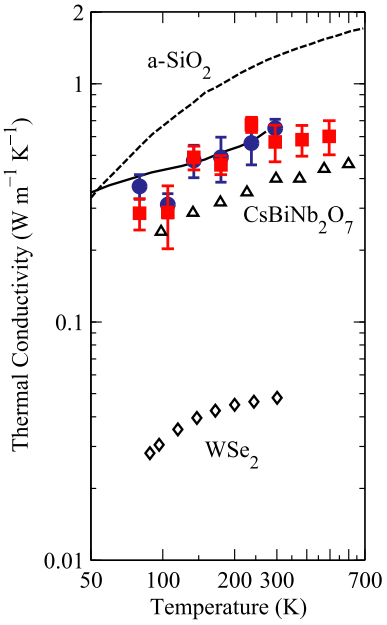

Fig. 3. Thermal conductivity versus temperature for two 5% La ($x = 0.1$) $Sr_{2-x}La_xNb_2O_{7-\delta}$ samples of different thicknesses; 130 nm (blue circles) and 800 nm (red squares). Literature data for amorphous SiO_2 [dashed line, Ref. (42)], bulk $Sr_5Nb_5O_{17}$ [solid line, Ref. (22)], $CsBiNb_2O_7$ [triangles, Ref. (18)] and WSe_2 [diamonds, Ref. (2)] are included for comparison.

[± 0.03 W· (m · K)$^{-1}$]. This value is of the same magnitude as the samples in both the thickness and doping series, thereby confirming that (a) the presence of minority fractions of the $Sr_5Nb_5O_{17}$ phase has minimal effect on the cross-plane κ, and (b) that the electrical contribution to κ as a result of La-doping coupled with different annealing conditions is dwarfed by the phonon contribution.

Additionally, in Fig. 2 we include the thermal conductivity along the *b*-axis of textured, hot-forged ceramic $Sr_{2-x}La_xNb_2O_{7-\delta}$ samples ($x = 0.01$) reported by Sparks *et al.* in Ref. [19]. We see a 40%–45% reduction in the κ of our thin films versus the bulk samples measured via thermal flash by Sparks.[19] We do not believe that this reduction is caused by film boundary scattering, since κ is independent of film thickness, as shown in Fig. 2. If boundary scattering were playing a role in the observed reduction, we would expect κ to increase with increasing film thickness, asymptotically approaching the bulk value from Ref. [19]. Similarly, we see no variation in κ due to different dopant concentrations of lanthanum, allowing us to conclude that neither impurity nor film boundary scattering are dominant phonon scattering mechanisms in these samples. Alternatively, phonons are more readily scattered at the weakly bonded interfaces normal to the measurement direction within the $Sr_2Nb_2O_7$ unit cell.

The difference in thermal conductivity along the *b*-axis of our films compared with the hot-forged ceramics reported by Sparks *et al.* likely stems from the degree of texture present in the different sample sets. The films we report here have significantly fewer non-0*k*0 peaks present in the X-ray diffraction pattern and the intensities of non-0*k*0 peaks relative to 0*k*0 peaks are lower than those reported by Sparks. Given the higher degree of crystallographic anisotropy present, we believe our lower thermal conductivity value stems from a higher degree of texture owing to sampling a high concentration of 0*k*0-oriented material.

We measured the thermal conductivity of two La-doped samples ($x = 0.1$) with different film thicknesses (130 and 800 nm, respectively) as a function of temperature from 80–500 K. Figure 3 is a plot of these data along with previous measurements of several materials, including those with weakly bonded, naturally layered structures as well as amorphous SiO_2 (a-SiO_2). Like the other layered structures shown in the figure, the thermal conductivities of both $Sr_{1.9}La_{0.1}Nb_2O_{7-\delta}$ films are less than a-SiO_2 across the temperature range, demonstrating the strong role that phonon scattering at weakly bonded layers can have on the thermal conductivity of crystalline materials. Additionally, our data show good agreement with cross-plane values for highly textured, bulk single-crystalline $Sr_5Nb_5O_{17}$ samples[22] (exclusively composed of $n = 5$ material in the $Sr_nNb_nO_{3n+2}$ homologous series; note that they use the nonstandard setting and that their *c*-axis is the *b*-axis in the standard setting) measured via a thermocouple-based, steady-state technique. Lastly, the thermal conductivity of $Sr_{1.9}La_{0.1}Nb_2O_{7-\delta}$ is larger than that of other layered material systems, including $CsBiNb_2O_7$[18] and WSe_2.[2] This is consistent with the fact that the cross-plane (*b*-axis) longitudinal speed of sound (v_L) in $Sr_2Nb_2O_7$ is 5192 m/s,[43] which is larger than the similarly directed sound velocities of the aforementioned materials [v_L equal to 3350 m/s from Ref. (18) and 1650 m/s from Ref. (2), respectively]. The differences in the cross-plane sound velocities of these materials can be attributed to the strength of the bonding between the layers; the bonds between WSe_2 layers being the weakest while those between "perovskite-slabs" in $Sr_{1.9}La_{0.1}Nb_2O_{7-\delta}$ being the strongest. The weaker bonds lead to stronger phonon scattering at the layer interfaces, leading to lower thermal conductivities.

To investigate the nature of thermal transport in our $Sr_{1.9}La_{0.1}Nb_2O_{7-\delta}$ layered structures, we turn to the minimum limit model for thermal conductivity.[44] Assuming an isotropic Debye solid, the expression for the minimum phonon thermal conductivity is

$$\kappa_{\min} = \frac{\hbar^2}{6\pi^2 k_B T^2} \sum_j \int_0^{\omega_{c,j}} \tau_{\min,j} \frac{\omega^4}{v_j} \frac{\exp\left[\frac{\hbar\omega}{k_B T}\right]}{\left(\exp\left[\frac{\hbar\omega}{k_B T}\right] - 1\right)^2} d\omega, \qquad (1)$$

where the summation is over the three acoustic phonon modes (one longitudinal, two transverse) and *j* denotes the particular mode, $\hbar$ is the reduced Planck's constant, ω is the phonon angular frequency, $\omega_{c,j}$ is the cutoff frequency, T is

the temperature, v_j is the phonon group velocity and $\tau_{min,j}$ is the minimum scattering time. To evaluate Eq. (1) for our material system, we use v_L = 5192 m/s from Ref. [43] and calculate $v_T = v_L\sqrt{(c_{55}/c_{22})}$ using literature values for the elastic constants[45] of $Sr_2Nb_2O_7$. Additionally, we use n = 72.993 nm^{-3} for the atomic density[19] of $Sr_2Nb_2O_7$ in calculating the cutoff frequencies ($\omega_{c,j} = v_j(6\pi^2 n)^{1/3}$).

Figure 4 shows our La-doped films of different thicknesses along with two versions of the model described by Eq. (1). The solid line is the Cahill-Watson-Pohl (CWP) model[44] and the dashed line is a modified version of the CWP that we refer to as the Layered model (LM).[46,47] Our LM calculations include the effects of scattering between weakly bonded layers. Like the work in Refs. [18] and [2], our data lie below the expected minimum thermal conductivity predicted by the CWP. The difference between the two models lies in the definition of τ_{min}; the CWP model defines the minimum scattering time to be one-half the period of oscillation between adjacent atoms in a given material, $\tau_{min,j,CWP}=\pi/\omega$. The LM incorporates an additional term via Matthiessen's rule[48] that accounts for scattering at the interface between two different layers. The minimum scattering time thus takes the form

$$\tau_{min,j,LM} = \left(\frac{\omega}{\pi} + v_j\frac{\pi^5 n}{\omega^2}\left(v_j - \frac{\omega d}{\pi}\right)^2\right)^{-1}, \quad (2)$$

where the first term is the scattering within the layers and the second is the scattering between layers, which is dependent on the separation distance, d. In the case of small d and weak bonding between layers (resulting in lower Debye cutoff frequencies), the difference between the modal sound speed and interlayer velocities is maximized, resulting in scattering times that approach the interatomic ones from CWP. The result is a reduction in the predicted minimum thermal conductivity due to the combined contributions of these separate scattering mechanisms. As we can see in Fig. 4, the LM lies below our measured data suggesting that the incorporation of interlayer scattering successfully establishes a new theoretical minimum thermal conductivity that is applicable to similarly layered structures.

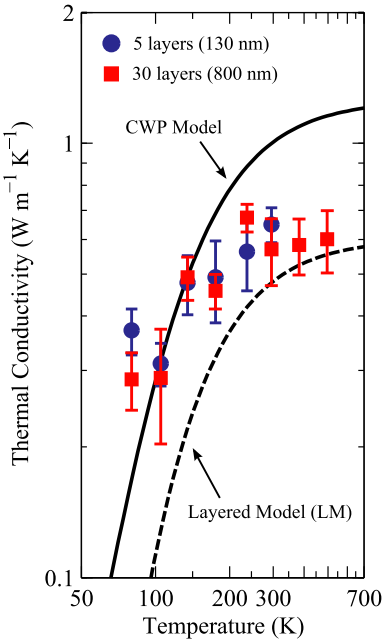

Fig. 4. Thermal conductivity versus temperature for two 5% La (x = 0.1) $Sr_{2-x}La_xNb_2O_{7-\delta}$ samples of different thicknesses plotted two models for the minimum thermal conductivity of a solid; the Cahill-Watson-Pohl (CWP) model[44] and a modified version of the CWP that includes the effects of scattering between weakly bonded layers (dashed line, this work).

IV. Conclusions

This work highlights several important features of the naturally layered $Sr_{2-x}La_xNb_2O_{7-\delta}$ material system that are relevant to a variety of application areas. First, we have shown that both the film thickness and lanthanum doping have little to no effect on the cross-plane (*b*-axis) thermal conductivity of the samples, indicating that the electrical and thermal properties of these films can be tuned independently over the doping range explored in this study. This conclusion is particularly significant in the scope of using strontium niobate as a high-temperature thermoelectric material. Second, the scalable-nature of the fabrication process used to synthesize these thin films and the exceptional degree of crystallinity and crystallographic texture confirmed via XRD and STEM is an extremely important component of this work. We have shown that the thermal conductivities of our CSD-fabricated thin films (0.6 $W \cdot (m \cdot K)^{-1}$) are comparable to that of similarly layered film structures created via epitaxial growth processes. The ability to fabricate these extremely insulative films through such a simple process both quickly and inexpensively on a broad variety of substrates without requiring lattice-matching epitaxy not only reinforces their potential as a commercial thermoelectric, but also as a next-generation thermal barrier coating to protect critical components in high-temperature operating environments.

Acknowledgments

B.M.F. is grateful for support from the ARCS Foundation Metro Washington Chapter. P.E.H. is appreciative for funding through the Army Research Office (W911NF-13-1-0378) and the NSF EAGER program (CBET-1339436). This work was performed in part at the Center for Atomic, Molecular, and Optical Science (CAMOS) at the University of Virginia. This work was supported, in part, by the Laboratory Directed Research and Development (LDRD) program at Sandia National Laboratories (H.B-S., M.J.C., D.L.M., P.G.C, J.F.I., P.E.H.). Sandia National Laboratories is a multi-program laboratory managed and operated by Sandia Corporation, a wholly owned subsidiary of Lockheed Martin Corporation, for the U.S. Department of Energy's National Nuclear Security Administration under contract DE-AC04-94AL85000. This project was supported by Financial Assistance Award No. 01-79-14214, awarded by U.S. Department of Commerce Economic Development Administration, to the University of Virginia (P.E.H, B.M.F). The content is solely the responsibility of the authors and does not necessarily represent the official views of the U.S. Department of Commerce Economic Development Administration.

References

[1]M. Dresselhaus, G. Chen, M. Tang, R. Yang, H. Lee, D. Wang, Z. Ren, J.-P. Fleuriall, and P. Gogna, "New Directions for Low-Dimensional Thermoelectric Materials," *Adv. Mater.*, **19** [8] 1043–53 (2007).

[2]C. Chiritescu, D. G. Cahill, N. Nguyen, D. Johnson, A. Bodapati, P. Keblinski, and P. Zschack, "Ultralow Thermal Conductivity in Disordered, Layered WSe_2 Crystals," *Science*, **315** [5810] 351–3 (2007).

[3]G. J. Snyder and E. S. Toberer, "Complex Thermoelectric Materials," *Nat. Mater.*, **7** [2] 105–14 (2008).

[4]O. Delaire, J. Ma, K. Marty, A. F. May, M. A. McGuire, M.-H. Du, D. J. Singh, A. Podlesnyak, G. Ehlers, M. D. Lumsden, and B. C. Sales, "Giant Anharmonic Phonon Scattering in PbTe," *Nat. Mater.*, **10** [8] 614–9 (2011).

[5]D. G. Cahill, "Extremes of Heat Conduction - Pushing the Boundaries of the Thermal Conductivity of Materials," *MRS Bulletin*, **37**, 855–63 (2012).

[6]J. C. Duda, P. E. Hopkins, Y. Shen, and M. C. Gupta, "Exceptionally Low Thermal Conductivities of Films of the Fullerene Derivative PCBM," *Phys. Rev. Lett.*, **110**, 015902 (2013).

[7]J. Ma, O. Delaire, A. F. May, C. E. Carlton, M. A. McGuire, L. H. VanBebber, D. L. Abernathy, G. Ehlers, T. Hong, A. Huq, W. Tian, V. M. Keppens, Y. Shao-Horn, and B. C. Sales, "Glass-Like Phonon Scattering from a Spontaneous Nanostructure in $AgSbTe_2$," *Nat. Nanotechnol.*, **8** [6] 445–51 (2013).

[8]C. J. Vineis, A. Shakouri, A. Majumdar, and M. G. Kanatzidis, "Nanostructured Thermoelectrics: Big Efficiency Gains from Small Features," *Adv. Mater.*, **22** [36] 3970–80 (2010).

[9]K. Koumoto, I. Terasaki, and R. Funahashi, "Complex Oxide Materials for Potential Thermoelectric Applications," *MRS Bull.*, **31** 206–10 (2006).

[10]B. M. Foley, H. J. Brown-Shaklee, J. C. Duda, R. Cheaito, B. J. Gibbons, D. Medlin, J. F. Ihlefeld, and P. E. Hopkins, "Thermal Conductivity of Nano-Grained $SrTiO_3$ thin films," *Appl. Phys. Lett.*, **101** [23] 231908 (2012).

[11]J. P. Feser, E. M. Chan, A. Majumdar, R. A. Segalman, and J. J. Urban, "Ultralow Thermal Conductivity in Polycrystalline CdSe Thin Films with Controlled Grain Size," *Nano Lett.*, **13** [5] 2122–7 (2013).

[12]D. L. Medlin and G. J. Snyder, "Interfaces in Bulk Thermoelectric Materials: A Review for Current Opinion in Colloid and Interface Science," *Curr. Opin. Colloid In.*, **14** [4] 226–35 (2009).

[13]K. Koumoto, Y. Wang, R. Zhang, A. Kosuga, and R. Funahashi, "Oxide Thermoelectric Materials: A Nanostructuring Approach," *Annu. Rev. Mater. Res.*, **40** [1] 363–94 (2010).

[14]G. Joshi, H. Lee, Y. Lan, X. Wang, G. Zhu, D. Wang, R. W. Gould, D. C. Cuff, M. Y. Tang, M. S. Dresselhaus, G. Chen, and Z. Ren, "Enhanced Thermoelectric Figure-of-Merit in Nanostructured p-Type Silicon Germanium Bulk Alloys," *Nano Lett.*, **8** [12] 4670–4 (2008).

[15]Z. Wang, J. E. Alaniz, W. Jang, J. E. Garay, and C. Dames, "Thermal Conductivity of Nanocrystalline Silicon: Importance of Grain Size and Frequency-Dependent Mean Free Paths," *Nano Lett.*, **11** [6] 2206–13 (2011).

[16]M. D. Losego, I. P. Blitz, R. A. Vaia, D. G. Cahill, and P. V. Braun, "Ultralow Thermal Conductivity in Organoclay Nanolaminates Synthesized Via Simple Self-Assembly," *Nano Lett.*, **13** [5] 2215–9 (2013).

[17]A. J. Minnich, M. S. Dresselhaus, Z. F. Ren, and G. Chen, "Bulk Nanostructured Thermoelectric Materials: Current Research and Future Prospects," *Energ. Environ. Sci.*, **2**, 466–79 (2009).

[18]D. G. Cahill, A. Melville, D. G. Schlom, and M. A. Zurbuchen, "Low Thermal Conductivity of $CsBiNb_2O_7$ Epitaxial Layers," *Appl. Phys. Lett.*, **96** [12] 121903 (2010).

[19]T. D. Sparks, P. A. Fuierer, and D. R. Clarke, "Anisotropic Thermal Diffusivity and Conductivity of La-Doped Strontium Niobate $Sr_2Nb_2O_7$," *J. Am. Ceram. Soc.*, **93** [4] 1136–41 (2010).

[20]A. Sakai, T. Kanno, K. Takahashi, Y. Yamada, and H. Adachi, "Large Anisotropic Thermoelectricity in Perovskite Related Layered Structure: $Sr_nNb_nO_{3n+2}$ (n=4,5)," *J. Appl. Phys.*, **108** [10] 103706 (2010).

[21]A. Sakai, T. Kanno, K. Takahashi, A. Omote, H. Adachi, and Y. Yamada, "Thermoelectric Responses in Layered Strontium-Niobates Via Two Ways of Charge Carrier Control Techniques," *J. Am. Ceram. Soc.*, **95** [5] 1750–5 (2012).

[22]W. Kobayashi, Y. Hayashi, M. Matsushita, Y. Yamamoto, I. Terasaki, A. Nakao, H. Nakao, Y. Murakami, Y. Moritomo, H. Yamauchi, and M. Karppinen, "Anisotropic Thermoelectric Properties Associated with Dimensional Crossover in Quasi-One-Dimensional $SrNbO_{3.4+d}$ ($d \sim 0.03$)," *Phys. Rev. B*, **84**, 085118 (2011).

[23]N. Ishizawa, F. Marumo, T. Kawamura, and M. Kimura, "The Crystal Structure of $Sr_2Nb_2O_7$, a Compound with Perovskite-Type Slabs," *Acta Crystallogr. B*, **31** [7] 1912–5(1975).

[24]R. W. Schwartz, "Chemical Solution Deposition of Perovskite Thin Films," *Chem. Mater.*, **9** [11] 2325–40 (1997).

[25]R. W. Schwartz, T. Schneller, and R. Waser, "Chemical Solution Deposition of Electronic Oxide Films," *CR Chim*, **7** [5] 433–61 (2004).

[26]X. Obradors, T. Puig, A. Pomar, F. Sandiumenge, S. Piñol, N. Mestres, O. Castaño, M. Coll, A. Cavallaro, A. Palau, J. Gázquez, J. C. González, J. Gutiérrez, N. Romà, S. Ricart, J. M. Moretó, M. D. Rossell, and G. van Tendeloo, "Chemical Solution Deposition: A Path Towards Low Cost Coated Conductors," *Supercond. Sci. Tech.*, **17** [8] 1055–64 (2004).

[27]M. J. Campion, H. J. Brown-Shaklee, M. A. Rodriguez, J. J. Richardson, P. G. Clem, and J. F. Ihlefeld, "Crystallization Atmosphere and Substrate Effects on the Phase and Texture of Chemical Solution Deposited Strontium Niobate Thin Films," *J. Am. Ceram. Soc.*, **96** [3] 743–9 (2013).

[28]D. G. Cahill, K. Goodson, and A. Majumdar, "Thermometry and Thermal Transport in Micro/Nanoscale Solid-State Devices and Structures," *J. Heat Transf.*, **124** [2] 223–41 (2002).

[29]P. E. Hopkins, L. M. Phinney, J. R. Serrano, and T. E. Beechem, "Effects of Surface Roughness and Oxide Layer on the Thermal Boundary Conductance at Aluminum/Silicon Interfaces," *Phys. Rev. B*, **82**, 085307 (2010).

[30]A. J. Schmidt, X. Chen, and G. Chen, "Pulse Accumulation, Radial Heat Conduction, and Anisotropic Thermal Conductivity in Pump-Probe Transient Thermoreflectance," *Rev. Sci. Instrum.*, **79** [11] 114902 (2008).

[31]D. G. Cahill, "Analysis of Heat Flow in Layered Structures for Time-Domain Thermoreflectance," *Rev. Sci. Instrum.*, **75** [12] 5119–22 (2004).

[32]C. Thomsen, J. Strait, Z. Vardeny, H. J. Maris, J. Tauc, and J. J. Hauser, "Coherent Phonon Generation and Detection by Picosecond Light Pulses," *Phys. Rev. Lett.*, **53**, 989–92 (1984).

[33]C. Thomsen, H. T. Grahn, H. J. Maris, and J. Tauc, "Surface Generation and Detection of Phonons by Picosecond Light Pulses," *Phys. Rev. B*, **34**, 4129–38 (1986).

[34]Y. Touloukian and E. Buyco, *Thermophysical Properties of Matter - Specific Heat: Metallic Elements and Alloys*, Vol 4. IFI/Plenum, New York, NY, 1970.

[35]J. Leitner, M. Hampl, K. Ruˇzˇicˇka, M. Straka, D. Sedmidubský, and P. Svoboda, "Heat Capacity, Enthalpy and Entropy of Strontium Niobate $Sr_2Nb_2O_7$ and Calcium Niobate $Ca_2Nb_2O_7$," *Thermochim. Acta*, **475** [1–2] 33–8 (2008).

[36]D.-W. Oh, J. Ravichandran, C.-W. Liang, W. Siemons, B. Jalan, C. M. Brooks, M. Huijben, D. G. Schlom, S. Stemmer, L. W. Martin, A. Majumdar, R. Ramesh, and D. G. Cahill, "Thermal Conductivity as a Metric for the Crystalline Quality of $SrTiO_3$ Epitaxial Layers," *Appl. Phys. Lett.*, **98** [22] 221904 (2011).

[37]H. C. Wang, C. L. Wang, W. B. Su, J. Liu, Y. Zhao, H. Peng, J. L. Zhang, M. L. Zhao, J. C. Li, N. Yin, and L. M. Mei, "Enhancement of Thermoelectric Figure of Merit by Doping Dy in $La_{0.1}Sr_{0.9}TiO_3$ Ceramic," *Mater. Res. Bull.*, **45** [7] 809–12 (2010).

[38]P. Daniels, R. Tamazyan, C. A. Kuntscher, M. Dressel, F. Lichtenberg, and S. van Smaalen, "The Incommensurate Modulation of the Structure of $Sr_2Nb_2O_7$," *Acta Crystallogr. B*, **58** [6] 970–6 (2002).

[39]T. Williams, F. Lichtenberg, D. Widmer, J. Bednorz, and A. Reller, "Layered Perovskitic Structures in Pure and Doped $LaTiO_{3.5-x}$ and $SrNbO_{3.5-x}$," *J. Solid State Chem.*, **103** [2] 375–86 (1993).

[40]F. Lichtenberg, A. Herrnberger, K. Wiedenmann, and J. Mannhart, "Synthesis of Perovskite-Related Layered $A_nB_nO_{3n+2} = ABO_x$ Type Niobates and Titanates and Study of Their Structural, Electric and Magnetic Properties," *Prog. Solid State Ch.*, **29** [1–2] 1–70 (2001).

[41]H. W. Schmalle, T. Williams, A. Reller, F. Lichtenberg, D. Widmer, and J. G. Bednorz, "A Novel Semiconducting Perovskite-Related Phase: $Sr_5Nb_5O_{17}$," *Acta Crystallogr. C*, **51** [7] 1243–6 (1995).

[42]D. G. Cahill, "Thermal Conductivity Measurement from 30 to 750 K: The 3 Omega Method," *Rev. Sci. Instrum.*, **61** [2] 802–8 (1990).

[43]G. Shabbir and S. Kojima, "Acoustic and Thermal Properties of Strontium Pyroniobate Single Crystals," *J. Phys. D*, **36** [8] 1036–9 (2003).

[44]D. G. Cahill, S. K. Watson, and R. O. Pohl, "Lower Limit to the Thermal Conductivity of Disordered Crystals," *Phys. Rev. B*, **46** 6131–40 (1992).

[45]M. Adachi, Y. Akishige, T. Asahi, K. Deguchi, K. Gesi, K. Hasebe, T. Hikita, T. Ikeda, Y. Iwata, M. Komukae, T. Mitsui, E. Nakamura, N. Nakatani, M. Okuyama, T. Osaka, A. Sakai, E. Sawaguchi, Y. Shiozaki, T. Takenaka, K. Toyoda, T. Tsukamoto, and T. Yagi, "$Sr_2Nb_2O_7$ [F], 8A-5"; in *Landolt-Bornstein - Group III Condensed Matter*, Vol. **36A2**, Edited by T. M. Y. Shiozaki, E. Nakamura. . Springer, Berlin, Germany.

[46]P. E. Hopkins and E. S. Piekos, "Lower Limit to Phonon Thermal Conductivity of Disordered, Layered Solids," *Appl. Phys. Lett.*, **94** [18] 181901 (2009).

[47]P. E. Hopkins and T. E. Beechem, "Phonon Scattering and Velocity Considerations in the Minimum Phonon Thermal Conductivity of Layered Solids Above the Plateau," *Nanosc. Microsc. Therm.*, **14** [1] 51–61 (2010).

[48]C. Kittel, *Introduction to Solid State Physics*, 7th edition. John Wiley and Sons, Inc., Hoboken, NJ, 1996. □